Electron-positron plasma drop formed by ultra-intense laser pulses

Inga Kuznetsova and Johann Rafelski

Electron-Positron Plasma Drop Formed by Ultra-Intense Laser Pulses

Inga Kuznetsova and Johann Rafelski

Department of Physics, The University of Arizona, Tucson, Arizona, 85721, USA

We study the initial properties, and positron annihilation within a small electron-positron plasma drop formed by intense laser pulse energy. Such QED cascade generated plasma is in general far below the chemical (particle yield) equilibrium. We find that the available electrons and positrons equilibrate kinetically, yet despite relatively high particle density the electron-positron annihilation is very slow suggesting a rather long lifespan of the plasma drop.

I. INTRODUCTION

Conversion of the high intensity laser pulse energy into a dense gas of e^+, e^- electron-positron pairs is a topic of current theoretical and, soon, experimental interest. A QED cascade mechanism producing a rapid conversion of laser pulse energy into pairs was demonstrated in [1] for pulse intensity on the order of 10^{24} W/cm². Considering the known reaction cross sections [2], subsequent to the electromagnetic cascade process discussed in Ref. [1], photons escape the small plasma drop, while as we show here, the electromagnetic scattering thermalizes the momentum distribution of this relatively dense electron-positron phase. We thus find a drop of 'thermal' momentum equilibrated, but 'chemical' yield non-equilibrated electron-positron plasma with size as small as a few μm and an energy content up to a kJ. Such plasma will expand, and loose energy by positron annihilation. We obtain here the rates of energy, and particle loss by annihilation.

The corresponding initial local energy density is provided by the laser field. We assume the formation of the plasma drop at rest in the lab frame e.g. invoking symmetric laser pulse collisions triggering QED cascades. The experimental pulse intensity parameter, defining plasma drop properties, is [3]

$$a_0 = \frac{eE_0\lambda}{m}, \tag{1}$$

where e is the electron charge, E_0 is the laser field strength in the focus, λ is the wavelength, and m is the electron (positron) mass. The discussion of physical properties, that we present, corresponds to $a_0 \simeq 4000$ This value will be within the range of the next generation ultra intense pulsed lasers. For a plasma drop radius $R = 3$ μm, $2R = 3\lambda$ the corresponding total plasma drop energy is $\mathcal{O}(0.3)$ kJ.

In the present context of plasma cooling we extended results of Ref. [2] to the lower density and lower temperature domain. Important theoretical refinement discussed here for the first time in context of laser generated low density e^-e^+-plasma is the consideration of the plasmon screening depending on plasma temperature and density. We also extend our earlier considerations to the nonrelativistic regime $T \leq m$ as required in the study of the

plasma expansion and freeze-out process.

In experimental conditions we consider here, all photons produced will escape from the small drop of low density plasma of electrons and positrons without much if any scattering. However, even far from chemical equilibrium density of particle pair yield, it is possible for the produced electrons and positrons to equilibrate thermally by means of Møller and Bhabha scattering

$$e^\pm + e^\pm \leftrightarrow e^\pm + e^\pm, \tag{2}$$
$$e^\pm + e^\mp \leftrightarrow e^\pm + e^\mp, \tag{3}$$

forming an electron-positron plasma drop: when the drop size R exceeds the scattering length L_{ee}

$$R > L_{ee}, \tag{4}$$

multiple scattering processes can occur allowing kinetic 'thermal' equilibration. We therefore study positron annihilation loss processes assuming the Fermi-Boltzmann energy distribution of available particles. We solve kinetic population equations and evaluate the fraction of particles in plasma which can annihilate during the plasma lifespan.

There are two paths to positron annihilation, the direct in-flight pair annihilation,

$$e^\pm + e^\mp \to \gamma + \gamma \tag{5}$$

and in flight bound state positronium p_s formation

$$e^\pm + e^\mp \to \gamma + \text{Pn} \qquad \text{Pn} \to n\gamma, \; n = 2, 3 \tag{6}$$

which is followed ultimately by annihilation. Annihilation life span of positronium for spin 0 is $\tau_{P2} = 0.12$ ns, while for spin 1 $\tau_{P3} = 140$ ns. However, positronium formation cross section only competes with the in-flight annihilation cross section for temperature below $T \approx 60$ eV [4], and at that point the expansion dilution will in general slow down considerably these processes.

In section II we present cross sections for Møller and Bhabha scattering including in the plasmon screening effects. We compare the resulting pair annihilation cross section with positronium formation. In section III we present numerical results for Møller and Bhabha scattering mean free path, and also annihilation relaxation time. We discuss conditions for plasma drop to be thermally equilibrated. In section IV we evaluate our results and present conclusions.

II. e^+, e^- PLASMA REACTION RATES

A. Scattering rates

1. Particle Density

We consider the case of a small non-opaque expanding electron-positron plasma drop. The drop stays thermally equilibrated by scattering processes. The electron (positron) multiplicity N_i ($i = e^+, e^-$) is thus in thermal (momentum distribution) but not in chemical (yield distribution) equilibrium.

It has been shown [5] that in order to maximize the entropy at fixed particle number the appropriate maximum entropy distribution is the usual Fermi-Dirac $f_{e,\bar{e}}$ distribution accompanied by a phase space occupancy parameter Υ

$$f_{e,\bar{e}} = \frac{1}{\Upsilon^{-1}e^{(u \cdot p \mp \nu)/T} + 1}. \tag{7}$$

$\Upsilon(t)$ describes the pair density and is in general a function of time, and is the same for both, particles and antiparticles. This is in contradistinction to the chemical potential ν which changes sign, $\nu_{\bar{e}} = -\nu_e$ comparing particles and antiparticles. Chemical potential ν regulates the abundance difference between particles and antiparticles and thus in general is only weakly dependent on time. A system with $\Upsilon = 1$ for all particles is in chemical equilibrium and we refer to particle density with $\Upsilon = 1$ as a chemical equilibrium density.

Note that the Lorentz-invariant exponents involve the scalar product of the particle 4-momentum p_i^μ with the local 4-vector of velocity u^μ, where u^μ describes local collective flow of matter as is expected for unconfined plasma drop. The thermal properties ν, T, Υ are defined in the local rest frame. In the absence of local matter flow the local rest frame is the laboratory frame

$$u^\mu = \left(1, \vec{0}\right), \qquad p^\mu = (E, \vec{p}). \tag{8}$$

We thus have

$$f_{e,\bar{e}} = \frac{1}{\Upsilon_{e,\bar{e}}^{-1}e^{E/T} + 1}, \quad \Upsilon_{e,\bar{e}} = \Upsilon e^{\pm\nu/T} \tag{9}$$

The yields of particles are

$$N_{e,\bar{e}} = n_{e,\bar{e}}V = g_{e,\bar{e}}V \int \frac{d^3p}{(2\pi)^3} f_{e,\bar{e}}, \tag{10}$$

where $V = 4\pi R^3/3$ is the volume, $g_{e,\bar{e}} = 2$ is the spin degeneracy. When the $e, \bar{e}$-pair yield is far below chemical equilibrium that is $\Upsilon \ll 1$ the effects of quantum statistics are in general less significant and Boltzmann limit is often equally precise

$$f_{e,\bar{e}} \to \Upsilon_{e,\bar{e}}e^{-E/T}. \tag{11}$$

2. Plasmon mass and screening length

To avoid Coulomb singularity in reaction matrix elements we introduce the plasmon mass, induced by plasma screening effect, following the example of gluon dynamics in quark-gluon plasma [6]. A plasmon mass is [7]

$$m_\gamma^2 = \omega_{pl}^2 = 8\pi\alpha \int \frac{f_{e^+} + f_{e^-}}{E_e}\left(1 - \frac{p^2}{3E_e^2}\right)\frac{dp^3}{(2\pi)^3}. \tag{12}$$

For non relativistic temperatures $T \ll m_e$, m_γ goes to classical plasma frequency, and a simple limit also emerges for relativistic temperatures with $\Upsilon = 1$,

$$m_\gamma \approx \begin{cases} 8\pi\alpha n_e/m_e & T < m_e, \\ \sqrt{4\pi\alpha}T/3 & T > m_e, \Upsilon = 1 \end{cases} \tag{13}$$

The corresponding screening length, the Debye radius, is

$$r_D = \frac{v_T}{\omega_{pl}}. \tag{14}$$

and the mean thermal particle velocity v_T is

$$v_T = \frac{\int \frac{p}{E}f d^3p}{\int f d^3p} \tag{15}$$

since $f_{e^+} = f_{e^-} = f$. We show in the figure 1 the electron (positron) screening length and the mass of plasmon as a function of T. Plasmon mass is increasing towards the small temperatures and is asymptotically constant, similar to the behavior of the plasma density. Screening length is otherwise decreasing towards the small temperatures (inverse proportional to m_γ and $v_T \propto \sqrt{T}$) in our range of temperature.

3. Boltzmann limit

We are interested in experimental conditions in which the number of pairs produced is large compared to residual electron density originating in matter. Further we will deal with conditions ($\Upsilon_e < 1$ or/and $T \leq m$ MeV) which allow to use the Boltzmann approximation. Then, we have

$$\frac{n_e - n_{\bar{e}}}{n_e + n_{\bar{e}}} \to \sinh(\nu/T) \ll 1. \tag{16}$$

In what follows we will set $\nu = 0$, and consider elsewhere the case for very low density degenerate plasma where chemical potential may become important. We thus have $\Upsilon_{e,\bar{e}} = \Upsilon$. In the relativistic Boltzmann (classical) limit the plasma density and energy density are

$$n_e = \frac{\Upsilon_e g_e T^3}{2\pi^2}x^2 K_2(x), \tag{17}$$

$$\epsilon = \Upsilon_e \frac{3g_e T^4}{2\pi^2}\left(x^2 K_2(x) + \frac{1}{3}x^3 K_1(x)\right), \tag{18}$$

where $K_i(x)$ is a Bessel function, $x = m/T$.
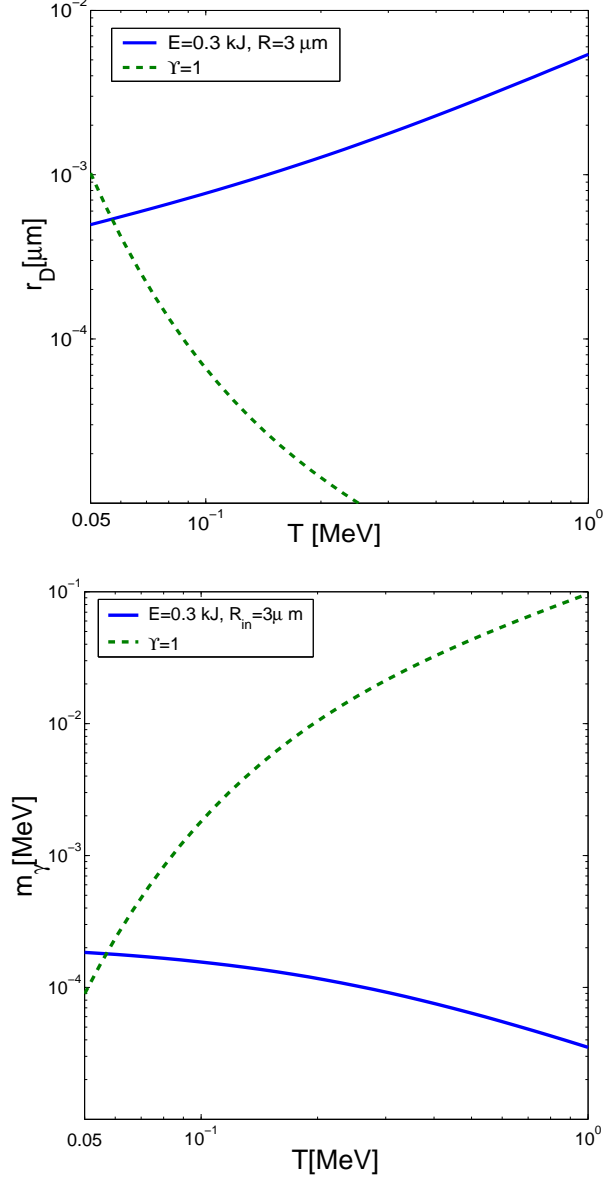
FIG. 1: Upper panel: electron (positron) screening length as a function of plasma temperature; Lower panel: mass of plasmon as a function of T.

4. Electron (positron) scattering rates

In the evaluation of matrix element we use Mandelstam variables: s, u, and t. In the case of Møller scattering

$$s = (p_1 + p_2)^2; \quad u = (p_3 - p_2)^2; \quad t = (p_3 - p_1)^2; \quad (19)$$

and $s + u + t = m_1^2 + m_2^2 + m_3^2 + m_4^2$.

The Møller scattering matrix element is [2, 8, 9],

$$|M_{e^\pm e^\pm}|^2 = 2^6 \pi^2 \alpha^2 \left\{ \frac{s^2 + u^2 + 8m^2(t - m^2)}{2(t - m_\gamma^2)^2} + \right.$$
$$\left. \frac{s^2 + t^2 + 8m^2(u - m^2)}{2(u - m_\gamma^2)^2} + \frac{(s - 2m^2)(s - 6m^2)}{(t - m_\gamma^2)(u - m_\gamma^2)} \right\} (20)$$

In the case of Bhabha scattering we have

$$s = (p_3 - p_2)^2; \quad u = (p_1 + p_2)^2; \quad t = (p_3 - p_1)^2, \quad (21)$$

see diagrams in [2]. The matrix element does not change in terms of variables p_1, p_2, p_3, when in variables s, u, t we need to cross u and s in Møller scattering matrix element, see Eq. (20),

$$|M_{e^\pm e^\mp}(s, t, u)|^2 = |M_{e^\pm e^\pm}(u, t, s)|^2; \quad (22)$$

thus we find

$$|M_{e^\pm e^\mp}|^2 = 2^6 \pi^2 \alpha^2 \left\{ \frac{s^2 + u^2 + 8m^2(t - m^2)}{2(t - m_\gamma^2)^2} + \right.$$
$$\left. \frac{u^2 + t^2 + 8m^2(s - m^2)}{2(s - m_\gamma^2)^2} + \frac{(u - 2m^2)(u - 6m^2)}{(t - m_\gamma^2)(s - m_\gamma^2)} \right\} (23)$$

For Møller and Bhabha scattering the cross section $\sigma_{ee}(s)$ can be obtained by averaging the matrix element over the t variable:

$$\sigma_{ee}(s) = \frac{1}{16\pi(s - 4m^2)^2} \int_{t_{\min}}^{t_{\max}} dt |M_{ee}|^2, \quad (24)$$

where $t_{\min} = -(s - 4m^2)$, $t_{\max} = 0$ in both cases [2]. Similar evaluations were done for heavy quarks production [10].

For Møller and Bhabha cross sections we obtain in plasma, keeping m_γ:

$$\sigma_{e^\pm e^\pm \leftrightarrow e^\pm e^\pm}(s) = \frac{1}{16\pi(s - 4m^2)^2} \int_{-(s-4m^2)}^0 dt |M_{e^\pm e^\pm}|^2 = \frac{4\pi\alpha^2}{(s - 4m^2)} \left(\frac{s^2 + 8m^2(m_\gamma^2 - m^2) + (s + m_\gamma^2 - 4m^2)^2}{(s + m_\gamma^2 - 4m^2) m_\gamma^2} + 1 \right)$$

$$+ \frac{8\pi\alpha^2}{(s - 4m^2)^2} \left(\frac{(s - 2m^2)(s - 6m^2)}{(s - 4m^2 + 2m_\gamma^2)} + s + m_\gamma^2 \right) \ln \frac{m_\gamma^2}{s - 4m^2 + m_\gamma^2}; \quad (25)$$

$$\sigma_{e^\pm e^\mp \leftrightarrow e^\pm e^\mp}(s) = \frac{1}{16\pi(s-4m^2)^2} \int_{-(s-4m^2)}^{0} dt |M_{e^\pm e^\mp}|^2 \;=\; \frac{2\pi\alpha^2}{(s-4m^2)} \times$$

$$\left[\frac{s^2 + 8m^2(m_\gamma^2 - m^2) + (s + m_\gamma^2 - 4m^2)^2}{\left(s + m_\gamma^2 - 4m^2\right) m_\gamma^2} + 1 + \frac{8\left((s-4m^2)^2 + m^2(s - m^2)\right)}{3(s - m_\gamma^2)^2} + \frac{3s + 2m_\gamma^2 + 4m^2}{(s - m_\gamma^2)} \right.$$

$$\left. + 2\,\frac{(m_\gamma^2 + s)^2 - 4m^4 + (s^2 - m_\gamma^4)}{(s - m_\gamma^2)} \ln \frac{m_\gamma^2}{s - 4m^2 + m_\gamma^2} \right]. \tag{26}$$

B. $e + \bar{e}$ Annihilation

1.   Master equation and annihilation time constant

The master population equation reads

$$\frac{1}{V}\frac{dN_{e,\bar{e}}}{dt} = -\Upsilon_e \Upsilon_{\bar{e}} W_{\mathrm{ann}}. \tag{27}$$

We have made explicit the dependence of evolution of the particle (pair) multiplicity in thin plasma on the prevailing density showing the factor $\Upsilon_e \Upsilon_{\bar{e}}$.

A simplification form of the Master equation (up to dilution by volume expansion, to be considered at another opportunity) is easily obtained

$$\frac{1}{\Upsilon_e}\frac{d\Upsilon_e}{dt} = -\frac{1}{\tau_{\mathrm{ann}}^e}\frac{\Upsilon_{\bar{e}}}{\Upsilon_{\bar{e}}^{\mathrm{in}}}, \tag{28}$$

introducing the annihilation relaxation time τ_{ann}^e [2]

$$\tau_{\mathrm{ann}}^e = \frac{dn_e/d\Upsilon_e}{\Upsilon_e^{\mathrm{in}} W_{\mathrm{ann}}}. \tag{29}$$

and similar for $\tau_{\mathrm{ann}}^{\bar{e}}$. In our case $\Upsilon_e \simeq \Upsilon_{\bar{e}}$ and we see that

$$\frac{\Upsilon_{\bar{e}}^{\mathrm{in}}}{\Upsilon_{\bar{e}}} = \int_0^t \frac{dt'}{\tau_{\mathrm{ann}}^{\bar{e}}}(t') \tag{30}$$

We can write a similar master equation for the plasma drop energy loss

$$\frac{1}{V}\frac{dE^{\mathrm{tot}}}{dt} = -\Upsilon_e \Upsilon_{\bar{e}} W_{\mathrm{ann}}^E, \tag{31}$$

where E^{tot} is the total energy of plasma drop. The relaxation time of energy loss is

$$\tau_{\mathrm{ann}}^E = \frac{d\epsilon/d\Upsilon_e}{\Upsilon_e^{\mathrm{in}} W_{\mathrm{ann}}^E}, \tag{32}$$

where ϵ is plasma energy density, Υ_e^{in} is initial electron (positron) phase space occupancy.

2.   Annihilation rate in-flight

When electrons collide with positrons they can annihilate. We consider here the dominant annihilation process in flight into two photons. The invariant rate of annihilation per unit of volume and time $e + \bar{e} \to \gamma + \gamma$ is $(3 + 4 \to 1 + 2)$

$$W_{\mathrm{ann}} = \frac{g_e^2}{2(2\pi)^8} \int \frac{d^3 p_1^\gamma}{2E_1^\gamma} \int \frac{d^3 p_2^\gamma}{2E_2^\gamma} \int \frac{d^3 p_3^e}{2E_3^e} \int \frac{d^3 p_4^{\bar{e}}}{2E_4^{\bar{e}}}$$

$$\times \delta^4\!\left(p_1^\gamma + p_2^\gamma - p_3^e - p_4^{\bar{e}}\right) \sum_{\mathrm{spin}} \left|\langle p_1^\gamma p_2^\gamma | M_{\gamma\gamma \leftrightarrow e\bar{e}} | p_3^e p_4^{\bar{e}}\rangle\right|^2$$

$$\times e^{u\cdot(p_1^e + p_2^e)/T} f_e(p_3^e)\Upsilon_e^{-1} f_4(p_4^{\bar{e}})\Upsilon_{\bar{e}}^{-1}. \tag{33}$$

Here $\langle p_1^\gamma p_2^\gamma | M_{\gamma\gamma \leftrightarrow e\bar{e}} | p_3^e p_4^{\bar{e}}\rangle$ is the annihilation quantum matrix element which we will consider in lowest order in fine structure constant $\alpha = e^2/4\pi = 1/137.036$; g_e is electron-positron degeneracy, and factor $1/2$ is due to the indistinguishability of the final state photons. We used this method to describe the electron-positron pair annihilation in [2], adapting it from work on strangeness production in quark-gluon plasma [11–14]. In the last line of Eq. (33) we introduce $\Upsilon_e^{-1}\Upsilon_{\bar{e}}^{-1}$ to compensate the factor seen in Eq. (27).

The invariant rate Eq. (33) relates to the electron-positron pair annihilation cross section [15], in Boltzmann limit we have

$$W_{\mathrm{ann}} = \frac{g^2 T}{32\pi^4} \int_{4m^2}^{\infty} ds \sqrt{s}(s - 4m^2)\, \sigma_{ee\to\gamma\gamma}(s) K_1(\sqrt{s}/T). \tag{34}$$

Here the annihilation cross section is [2]

$$\sigma_{ee\to\gamma\gamma}(s) = \frac{2\pi\alpha^2(s^2 + 4m^2 s - 8m^4)}{s^2(s - 4m^2)} \times$$

$$\left(\ln \frac{\sqrt{s} + \sqrt{s - 4m^2}}{\sqrt{s} - \sqrt{s - 4m^2}} - \frac{(s + 4m^2)\sqrt{s^2 - 4m^2 s}}{(s^2 + 4m^2 s - 8m^4)} \right). \tag{35}$$

3.   Energy loss

Once in-flight $e + \bar{e}$ annihilation occurs, the produced photons escape the small plasma volume. An analogous

expression to Eq. (33) describes the energy loss rate due to pair annihilation

$$W_{ann}^E = \frac{g_\gamma^2}{2(2\pi)^8} \int \frac{d^3 p_1^\gamma}{2E_1^\gamma} \int \frac{d^3 p_2^\gamma}{2E_2^\gamma} \int \frac{d^3 p_3^e}{2E_3^e} \int \frac{d^3 p_4^e}{2E_4^e} \times$$

$$\times \delta^4 \left(p_1^\gamma + p_2^\gamma - p_3^e - p_4^e \right) \sum_{\text{spin}} |\langle p_1^\gamma p_2^\gamma | M_{ee \to \gamma\gamma} | p_3^e p_4^e \rangle|^2$$

$$\times (E_3^e + E_4^{\bar{e}}) f_e(p_3^e) f_4(p_4^e) \Upsilon_e^{-2} e^{u \cdot (p_1^\gamma + p_2^\gamma)/T}, \qquad (36)$$

We now obtain a relation analogous to Eq. (34). Consider the integral [15] leading to Eq. (34)

$$\int d^4 p \, e^{-\beta p \cdot u} \delta_0(p^2 - s) = \frac{2\pi}{\beta} \sqrt{s} K_1(\beta \sqrt{s}), \qquad (37)$$

where $u = (1, \vec{0})$ in lab frame. Instead, we now need to use

$$\int d^4 p \, p \cdot u \, e^{-\beta p \cdot u} \delta_0(p^2 - s) = -\frac{\partial}{\partial \beta} \frac{2\pi}{\beta} \sqrt{s} K_1(\beta \sqrt{s}). \qquad (38)$$

We use $d[K_1(x)/x]/dx = -K_2(x)/x$ to obtain

$$W_{ann}^E = \frac{g^2 T}{32\pi^4} \int_{s_{th}}^\infty ds\, s(s - 4m^2) \, \sigma_{ee \to \gamma\gamma}(s) K_2(\sqrt{s}/T). \qquad (39)$$

4. Positronium formation

The cross section for radiative positronium ($e\bar{e}$) formation, $e^- + e^+ \leftrightarrow \gamma + (e\bar{e})$ [16] is

$$\sigma_{pos} = \frac{2^{12}\pi^2 \omega}{3pm^2} \xi \left(\frac{\xi^2}{1 + \xi^2} \right)^3 \frac{e^{-4\xi \text{arccot}\xi}}{1 - e^{-2\pi\xi}} \left(1 + \frac{\omega^2(1 - \xi^2)}{5p^2} \right), \qquad (40)$$

where $\xi = \alpha m/2p$ and photon energy ω is defined by the conservation low

$$\omega + \frac{\omega^2}{4m} = p^2/m + \alpha^2 m/4. \qquad (41)$$

p is electron(positron) momentum in center of mass reference frame, $p = \sqrt{s - 4m^2}/2$. The Eq.(40) is valid while $\xi \le 1$. This condition is satisfied up to temperature on the order of 10 eV.

We did not consider in detail the influence of plasma screening on positronium formation, a topic which invites further work in view of currently available results. It was found in [17] that the plasma screening and collective effects significantly reduce the radiative recombination cross section in non ideal plasma. The screening effect for positronium formation should be similar to result for free electron radiative recombination with ions in non ideal classical plasmas. However, in positron - hydrogen plasma the Debye screening can result in a large increase of positronium formation cross section at incident positron energy 20-100 eV [18].

III. RESULTS FOR LASER FORMED PLASMA

A. Parameters for thermal plasma drop

We assume here that the total energy E of (colliding) laser pulses converts in the initial volume V to the e^+e^--plasma drop energy. The initial energy density $\epsilon = E/V$ is obtained from Eq.(1), and is characterized by a_0 and λ

$$\epsilon = \frac{1}{4\pi} E_0^2 = \frac{1}{4\pi} \left(\frac{a_0 m}{e\lambda} \right)^2. \qquad (42)$$

The phase space occupancy of plasma drop is

$$\Upsilon_e = \frac{1}{4\pi \epsilon_0(T)} \left(\frac{a_0 m}{e\lambda} \right)^2, \qquad (43)$$

where we introduced the chemical equilibrium energy density $\epsilon_0 = \epsilon|_{\Upsilon_e=1}$, Eq.(18). Then the total energy of plasma, E, is defined by plasma drop radius R for given parameter a_0 and wave length λ. Initial plasma size is expected to be close to the wavelength . We take the wavelength $R = 3\lambda/2$ for all cases considered below.

In figure 2 we show phase space occupancy Υ_e from Eq.(43) (upper panel) and corresponding plasma density n_{pl} (lower panel). The solid (blue) line shows actual chemical non-equilibrium value. For comparison the chemical equilibrium results are shown by dashed (green) line. We note that for $T >> 0.06$ MeV the fully equilibrated yield is much greater than what we can make using near future high intensity laser. However, the density of particles in plasma which we achieve is very high.

At $T << m$, when plasma becomes non-relativistic the energy/particle $\to mc^2$ is a constant and does not depend much on plasma temperature. Hence, the plasma particle density goes for $T \to 0$ to a constant for a given fixed energy and plasma drop size,

$$n_{\text{pl}} = n_e + n_{\bar{e}} = \frac{\epsilon}{mc^2}. \qquad (44)$$

and temperature can not be determined considering a given available energy constraint.

In a system where particle (pairs) can be produced but energy is fixed the entropy density reaches maximum at $\Upsilon = 1$. We show the entropy density of electron - positron plasma,

$$s = \int \frac{d^3 p}{2\pi^3} \left((f_e - 1) \ln(1 - f_e) - f_e \ln(f_e) \right), \qquad (45)$$

at $E = 0.3$ kJ and $R = 3\,\mu$m as a function of temperature in Fig. 3. As expected the maximum of entropy density is at the same temperature, $T = 0.06$ MeV, where phase space occupancy of electron and positron $\Upsilon_e = 1$. However, the maximum is very flat. Note that there is much less entropy density when the system is formed at relatively high temperature. This is so since there are fewer particle pairs and, for a relativistic gas, the entropy per
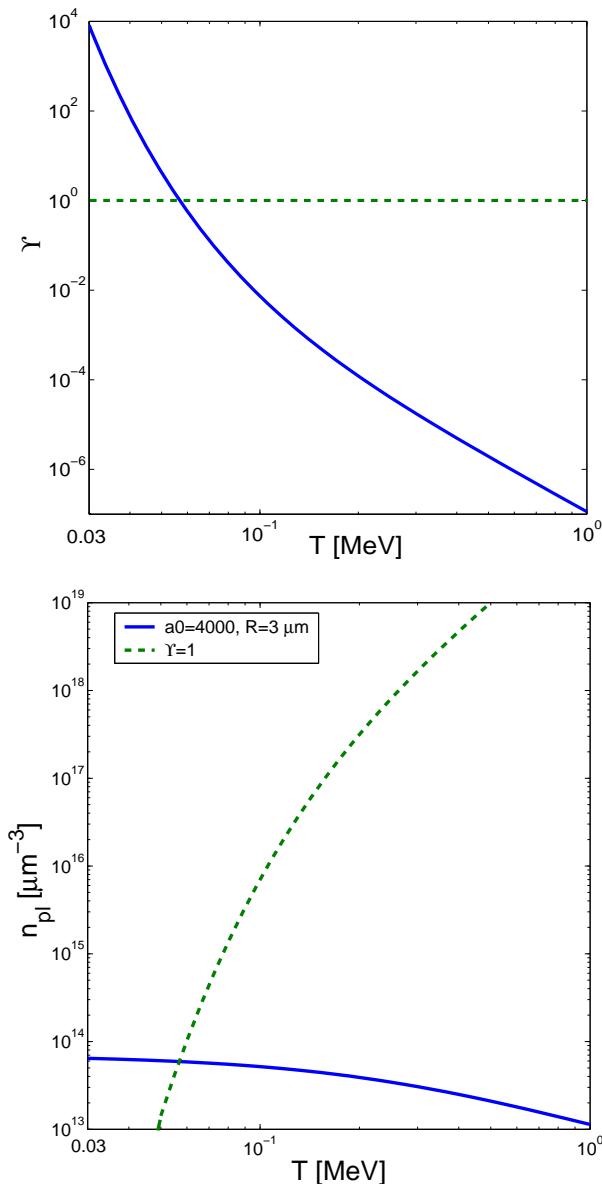
FIG. 2: Upper panel: electron (positron) phase space occupancy Υ_e as a function of T for $a_0 = 4000$ and $R = 3$ μm (solid, blue line); Lower panel: plasma density corresponding to phase space occupancy on upper panel (solid, blue line) and equilibrium density $\Upsilon = 1$ (dashed, green line) as a function of T.

FIG. 3: The entropy density of electron-positron plasma with $a_0 = 4000$ and $R = 3$ μm is shown as a function of temperature.

B. Electron and positron scattering

The formation of electron-positron plasma is further subject to the opacity condition Eq.(4). To check if this condition is satisfied we extend our earlier considerations [2] now introducing plasmon mass, Eq.(12) in a domain of mild relativistic and non relativistic temperatures.

The electron (positron) mean free path follows from

$$L_{ee} = \frac{n_e}{W_{ee}}, \tag{46}$$

where for scattering rate W_{ee} we use equation similar to Eq.(34) (since final state does not have two identical bosons the normalization factor is different).

$$W_{ee} = \frac{g^2 T}{32\pi^4} \int_{4m^2}^{\infty} ds \sqrt{s}(s - 4m^2) \, \sigma_{ee}(s) K_1(\sqrt{s}/T), \tag{47}$$

and

$$\sigma_{ee} = \sigma_{e^+e^+ \leftrightarrow e^-e^-} + \sigma_{e^-e^+ \leftrightarrow e^+e^-}. \tag{48}$$

In figure 4 we show electron (positron) scattering length L_{ee}, Eq.(46), at a given plasma radius $R = 3$ μm and energy 0.3 kJ ($a_0 = 4000$) as a function of plasma temperature T. Υ varies for every value of T as we see in figure 2. Since $\Upsilon_e \ll 1$ the scattering length can be evaluated in Boltzmann limit in practically the entire temperature range of interest, including $T > m$. We also show (dashed green line) for comparison the case $\Upsilon_e = 1$, that means that we allow the density to go up significantly and the small difference we see in figure 4 for high T is due to quantum gas properties.

particle is near to $S/N \simeq 4$. For low density far off equilibrium systems the expansion of the volume is thus accompanied by reactions that tend to chemically equilibrate the system and move it towards chemical equilibrium.
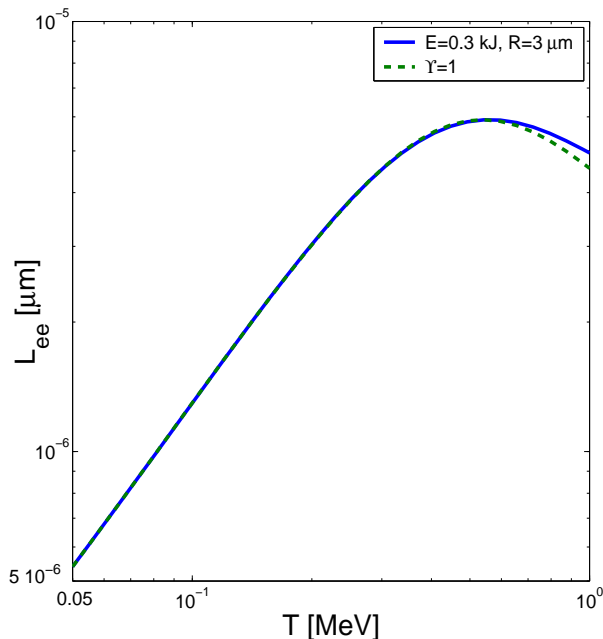
FIG. 4: Electron (positron) scattering length at given plasma radius and energy as a function of T.

At relativistic temperature $T \simeq 1$ MeV our present result is in agreement with scattering rates evaluated with plasmon mass taken in the limit of ultra relativistic temperatures in [2] with accuracy of few percents.

For constant plasma drop energy scattering length L_{ee} has maximum at $T \approx m$. In whole temperature range the plasmon mass is small and the first term in Eq. (25) and Eq. (26) is dominant, resulting in cross section for electron or positron scattering

$$\sigma_{ee} \propto m_\gamma^{-2} \propto n_e^{-1}. \qquad (49)$$

In the range where condition Eq. (49) is valid the electron (positron) mean free path does not depend on density or Υ_e. When the mean free path is increasing with decreasing density, this is compensated by larger cross section because of a smaller plasma screening effect or smaller m_γ. For the entire T range, the scattering length scale is a tiny fraction of the plasma size.

In temperature range $T < m$ the contribution of $4p^2 = s - 4m^2$ is much smaller than m^2 and much larger than m_γ^2 the approximate cross sections for Moller and Bhabha scatterings, Eq. (25) and Eq. (26) are

$$\sigma_{e^\pm e^\pm \leftrightarrow e^\pm e^\pm}(s) = 2\sigma_{e^\pm e^\mp \leftrightarrow e^\pm e^\pm}(s) = \frac{64\pi\alpha^2}{(s-4m^2)^2}\frac{m^4}{m_\gamma^2}. \qquad (50)$$

One can also consider Rutherford-type differential cross section for Møler scattering is [9]

$$\frac{d\sigma}{d\cos\theta} = \frac{\pi\alpha^2 m^2}{4p^4}\mathrm{cosec}^4\theta/2. \qquad (51)$$

We checked integrating Eq.(51) numerically that our Eq.(50) corresponds to total cross section from integrated Eq.(51) with cutoff angle $\theta_{\min} = m_\gamma/m$.

We found from the results presented in Fig. 4 that condition 4 is satisfied for all temperature range considered. We conclude that electron positron plasma drop can stay thermally equilibrated at relatively low densities when or $\Upsilon << 1$ and/or temperature $T << m$: the electron positron mean free path decreases when temperature decreases below electron mass because of factor $s - 4m^2 = 4p^2$ in denominator of cross section Eq. (50). At a temperature higher than m the other terms begin to contribute in cross sections Eq. (25) and Eq. (26). The electron positron mean free path decreases again.

The cross section, Eq (50), is valid in temperature range

$$T_{cr} = \frac{2\pi\alpha n_e}{m^2} < T < m, \qquad (52)$$

The reader should keep in mind that the present considerations do not automatically apply to the case of a degenerate electron-positron gas (high density or/and low temperature), where we should extend the investigation of collective plasmon dynamics in order to obtain a valid estimate of the electron positron scattering cross section.

C. Annihilation

1. Plasmons

While screening and plasma oscillations impact the scattering processes, this is not the case for our domain in regard to the annihilation process. There are several processes to consider:

1. The electron (positron) thermal mass correction, which is on the order of magnitude of m_γ. However, $m_\gamma << m_e$ and this correction is small.

2. Plasmon $\leftrightarrow e^+e^-$, when the reaction threshold is exceeded, $m_\gamma > 2m_e$ [6]. This can only happen at ultra relativistic temperatures. In the case considered here with constant plasma energy, $m_\gamma^2 \propto T^{-1}$ see figure 1, the threshold condition cannot be satisfied.

3. The hard photons from annihilation ($k \approx m$) can also rescatter on plasmons. The condition when screening has noticeable effect on photon propagation is [19]

$$kr_D \leq 1, \qquad (53)$$

where k is photon wave number and r_D is Debye radius Eq.(14). This condition is equivalent to condition $T < T_{cr}$, Eq.(52). We do not consider here such low temperature plasma.
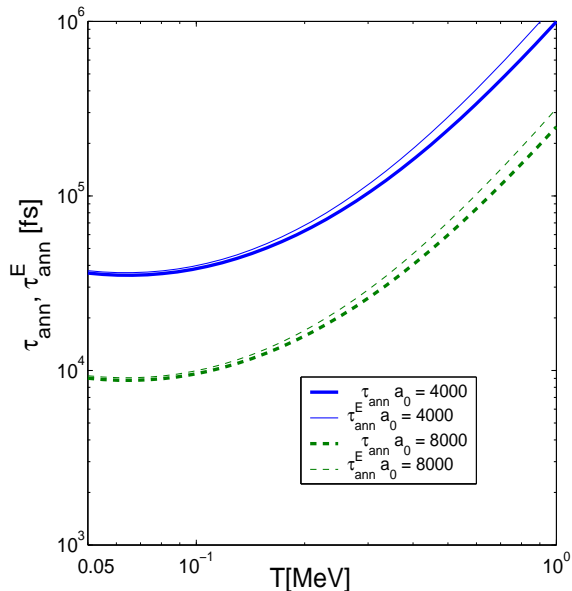
FIG. 5: Time constant for particle annihilation (thick lines) and energy loss (thin lines) at $a_0 = 4000, E = 0.3\,\mathrm{kJ}$ (solid blue lines) and $a_0 = 8000, E = 1.2\,\mathrm{kJ}$ (dashed green lines) as a function of plasma drop temperature.

2. Annihilation lifespan

We determine using the perturbative QED reaction rate the annihilation rate of plasma under conditions considered in previous subsections. We assume that the plasma drop formation lifespan is on the order of magnitude of laser pulse duration, 10 fs and this is the stage at which the density of pairs and thus annihilation should have the largest rate, however this is not the case since as T increases, pair density drops given the constant initial total energy, and thus the annihilation relaxation time increases.

In figure 5 we show relaxation times τ for particle number annihilation τ_{ann} (thick lines) and energy loss $\tau_{\mathrm{ann}}^{\mathrm{E}}$ (thin lines) for plasma at $a_0 = 4000$, $E = 0.3$ kJ (solid, blue lines) and $a_0 = 8000$, $E = 1.2$ kJ (green, dashed, lines) as a function of temperature. The values of τ are indeed largest for initial highest temperatures and there is a shallow minimum at $T \approx 0.065$ MeV. At $T < 0.065$ MeV the pair density is approximately constant but particle temperature decrease results to increase of annihilation relaxation time. The fastest annihilation occurs here because we have at this low temperature the highest mobility of particles at high density.

We recognize that the fraction of annihilations is very small initially, we obtain from Eq.(27)

$$N_{\mathrm{ann}}/N_0 \approx \Upsilon_{\mathrm{e}}^2 W_{\mathrm{ann}} \frac{t}{n_0} \approx \frac{t}{\tau_{\mathrm{ann}}}. \tag{54}$$

Another way to look at the conditions of annihilation is to note that relaxation time is inversely proportional to Υ_{e}. Then from Eq.(42) we have

$$\tau_{\mathrm{ann}} \propto \frac{\lambda^2}{a_0^2}, \tag{55}$$

which explains the dependence on a_0 we see in figure 5.

We see in figure 5 that the energy loss relaxation time τ_{ann}^E becomes very close to τ_{ann} for $T < m$. This is because the energy of plasma drop changes mostly because of pair mas disappearance and resulting plasma mass decrease. At $T > 2m$, energy loss relaxation time is as expected above annihilation relaxation time. This happens since there is preference for slower particles to annihilate and thus on average in thermal bath the particles or higher energy remain and annihilation leads to a slight increase of ambient plasma temperature.

Our result seen in figure 5 implies that the annihilation process even at highest initial density is a relatively slow compared to other dynamical effects controlling plasma drop: the plasma drop must live $t >> \tau_{ann}$ to have most positrons in plasma annihilated. This time is much longer than pulse duration, 10 fs, indeed it is on the scale of nano seconds. There is furthermore the kinetic expansion leading to further dilution of the plasma – when plasma drop expands with time the density decreases and the annihilation relaxation becomes even longer. Most if practically not all annihilation events, $3\,10^{-4} - 10^{-5}$ originate in the most dense plasma stage during laser pulse and reliable prediction of total annihilation yield require detailed control of the kinetic processes in the initial state of the plasma as well as precise understanding of the plasma drop expansion dynamics which further reduces annihilation rate ultimately leading to a cloud of streaming electron and positrons.

3. Inflight annihilation compared to positronium formation

In Fig. 6 we compare the nonrelativistic limit of the annihilation in flight cross section (dashed) to the cross section for radiative positronium ($e\bar{e}$) formation (solid, blue) as a function of electron(positron) kinetic energy in the center of mass frame $E_{\mathrm{kin}} = (s - 4m^2)/8m$. The cross sections intersect at $E_{\mathrm{kin}} \approx 150$ eV. This corresponds to cross-over temperature obtained in [4], $T_e \simeq 60$ eV. Thus the direct annihilation dominates down to this low temperature, and our prior results apply for $T > T_e$. For $T < T_e$ we have significant positronium formation only if we reach this condition without much of expansion which is not part of our present study.

IV. CONCLUSIONS

The key result of this study is that high intensity QED cascading leads to an electron-positron drop which does not annihilate but thermally equilibrate. In this plasma drop electron - positron pairs are thermalized by Møller
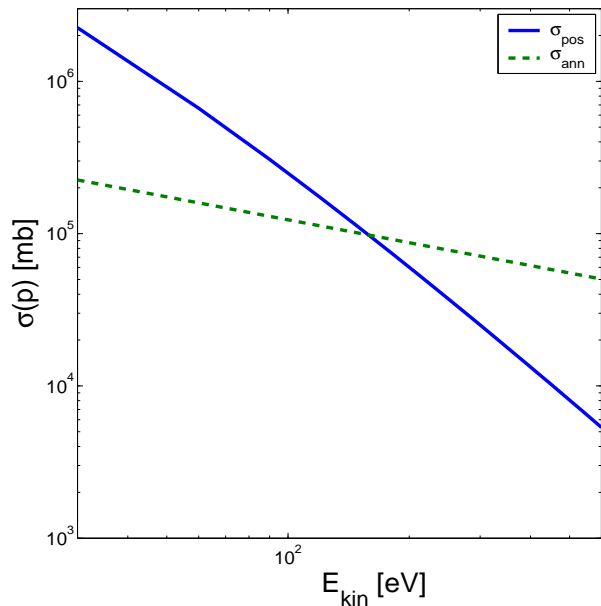
FIG. 6: Radiative positronium formation (solid line) and direct annihilation cross sections (dashed) as a functions of electron(positron) kinetic energy in the two particle center of momentum frame.

Eq.(2) and Bhabha Eq.(3) scattering, and annihilate very slowly, see figure (5).

We find that in Boltzmann limit the electron and positron scattering length nearly does not depend on plasma density at given temperature range due to collective plasmon effects. The cross section decrease at lower density is compensated by plasmon charge screening in the less dense plasma. As the result electron positron plasma can be thermally equilibrated at density and temperature range considered, far below chemical equilibrium of pair yield, $\Upsilon = 1$. The plasma drop size allows very many scattering process, we did not find any re-

striction on minimum plasma drop energy and/or maximum drop size considering opaqueness condition Eq.(4) for electron (positron) scattering.

We calculated as an example the annihilation relaxation time for an internal plasma drop energy $0.3 - 1.2$ kJ and radius 3 μm. Due to relatively low density the annihilation relaxation time is much longer than pulse duration, which is ≈ 10 fs. We obtained that 'in flight' annihilation is fastest at $T = 0.065$ MeV, yet still relatively slow. The radiative positronium production process exceeds the 'in flight' annihilation at much lower temperature, 60 eV, leading perhaps to the formation of positronium in late stages of the drop. If such low temperature is reached without drastic expansion dilution, very many positronium can be formed and positronium formation prolongs the lifespan of positrons, though the nature of the plasma drop is now different.

The experimental conditions will determine at what temperature and importantly for the following argument, rapidity, relative to the laboratory frame of reference the electron-positron drop will be formed [20, 21]. Multipulse arrangements can be easily obtained resulting in the plasma drop being formed at high rapidity. The greater the rapidity, the greater will be the effect of time dilation that prolongs the life span of the plasma drop as seen in the laboratory. We recognized in this work the relative stability against annihilation evaluated in the intrinsic rest frame of the drop. Therefore it appears possible to create using high density lasers a quasi-stable matter-antimatter plasma drop capable to travel macroscopic distances before dissipating into a low density cloud of particles.

[1] E. N. Nerush, I. Y. Kostyukov, A. M. Fedotov, N. B. Narozhny, N. V. Elkina and H. Ruhl, Phys. Rev. Lett. **106**, 035001 (2011) [Erratum-ibid. **106**, 109902 (2011)] [arXiv:1011.0958 [physics.plasm-ph]].

[2] I. Kuznetsova, D. Habs and J. Rafelski, Phys. Rev. D **81**, 053007 (2010) [arXiv:0911.0118 [physics.plasm-ph]].

[3] T. Tajima and G. Mourou Phys. Rev. ST Accel. Beams **5**, 031301 (2002).

[4] R.J. Gold, Astrophysical Journal, Part 1, **344** (1989), 232-238.

[5] J. Letessier, J. Rafelski and A. Tounsi, Phys. Rev. C **50**, 406 (1994) [arXiv:hep-ph/9711346].

[6] T. S. Biro, P. Levai and B. Muller, Phys. Rev. D **42**, 3078 (1990).

[7] M. B. Kislinger and P. D. Morley, Phys. Rev. D **13**, 2765 (1976).

[8] A. G. Aksenov, R. Ruffini and G. V. Vereshchagin, Phys. Rev. D **79**, 043008 (2009) [arXiv:0901.4837 [astro-ph.HE]].

[9] F. Halzen and A. D. Martin, "Quarks And Leptons: An Introductory Course In Modern Particle Physics," *New York, Usa: Wiley (1984) 396p*

[10] B. L. Combridge, Nucl. Phys. B **151**, 429 (1979).

[11] J. Rafelski, B. Muller, Phys. Rev. Lett. **48**, 1066 (1982).

[12] P. Koch, B. Muller, J. Rafelski, Z. Phys. **A324**, 453-463 (1986).

[13] T. Matsui, B. Svetitsky and L. D. McLerran, Phys. Rev. D **34**, 783 (1986) [Erratum-ibid. D **37**, 844 (1988)].

[14] P. Koch, B. Muller and J. Rafelski, Phys. Rept. **142**, 167 (1986).

[15] Jean Letessier, and Johann Rafelski *Hadrons and Quark-Gluon Plasma* (Cambridge University Press 2005), ISBN-10: 0521018234.

[16] A.I. Akhiezer, N.P. Merenkov, J. Phys. B: at Mol. Opt. Phys. **29**, 2135, (1996).

[17] Y.D. Jung, Phys. Plasmas 9, 4402, (2002).

[18] S. Sen, P. Mandal, P.K Mukherjee, Eur. Phys. J. D, **62** 379, (2011).

[19] S. H. Glenzer, H. J. Lee, P. Davis, T. Døppner, R.W.Falcone, C. Fortmann, B.A.Hammel, A.L.Kritcher, O.L.Landen, R.W.Lee, D.H.Munro, R.Redmer and S.Weber High Energy Density Physics **6**, (2010).

[20] L. Labun and J. Rafelski, Phys. Rev. D **84**, 033003 (2011) [arXiv:1102.5773 [hep-ph]].

[21] L. Labun and J. Rafelski, arXiv:1107.6026 [hep-ph].